Experimental Report

Proposal: **7-01-367** **Council:** 10/2012

Title: Phonon dispersion of (1-x)Bi1/2Na1/2TiO3-xBaTiO3 of different composition

This proposal is a new proposal

Researh Area: Materials

Main proposer: **PFORR Florian**

Experimental Team: PFORR Florian
DONNER Wolfgang
MAJOR Marton

Local Contact: IVANOV Alexandre

Samples: Bi1/2Na1/2TiO3
0.96Bi1/2Na1/2TiO3-0.04BaTiO3
0.88Bi1/2Na1/2TiO3-0.12BaTiO3

Instrument	Req. Days	All. Days	From	To
IN8	10	7	27/05/2013	03/06/2013

Abstract:

The structural phase transitions of the lead-free relaxor ferroelectric Bi1/2Na1/2TiO3 (BNT) have been investigated using various methods, but the understanding of the lattice dynamics is still very limited. Solid solutions like (1-x)Bi1/2Na1/2TiO3-xBaTiO3 (BNT-100xBT, BNT-BT) show particularly promising ferroelectric properties near the morphotropic phase boundary around BNT-6BT and should replace some lead-containing ferroelectric materials for environmental and health reasons in the medium term. However, a better understanding of the lattice dynamics is crucial for the determination of the influence of dopants like BaTiO3 on the crystal lattice of BNT. This influence needs to be understood before a systematic search for improvements in the ferroelectric and ageing properties can be conducted. Consequently, we propose to measure the phonon dispersion of BNT, BNT-4BT and BNT-12BT in the [100] direction. This pilot experiment, which is part of the PhD work of Florian Pforr, would also help us estimate the potential value of further inelastic neutron scattering measurements on BNT-BT at elevated temperature.

Phonon dispersion of $(1-x)$$Bi_{1/2}Na_{1/2}TiO_3$-$x$$BaTiO_3$ of different composition

F. Pforr, M. Major, W. Donner
Technische Universität Darmstadt, Institute of Materials Science, Alarich-Weiss-Straße 2, D-64287 Darmstadt, Germany

Introduction

Lead-containing ferroelectrics like $Pb_xZr_{1-x}TiO_3$ should be replaced by lead-free systems in the medium term. The future perspectives of lead-free ferroelectrics have been described by Rödel et al. [1]. One promising candidate is the solid solution of $Bi_{1/2}Na_{1/2}TiO_3$ (BNT) and $BaTiO_3$ (BT), designated as $(1-x)Bi_{1/2}Na_{1/2}TiO_3$-$x$$BaTiO_3$ (BNT-$100x$BT, BNT-BT), which was first reported by Takenaka et al. [2]. The ferroelectric parameters of solid solutions near the morphotropic phase boundary (MPB) around BNT-6BT were cited as $d_{33} = 125\,\mathrm{pC\,N^{-1}}$ and $\epsilon_{33}^T/\epsilon_0 = 580$ [1]. The structural phase transitions of BNT have been investigated in detail, but the understanding of the coherent and incoherent lattice dynamics is still very limited. However, a better understanding is crucial for the determination of the influence of dopants in BNT-based solid solutions. Consequently, we have measured the transverse phonon dispersion of BNT-4BT along different high symmetry directions at 300 K at IN8. Due to the expected temperature dependence of potential soft phonon modes, we have made additional measurements in the [$\xi\xi\xi$] direction at 100 K. (Pseudocubic indexation with a lattice parameter of approximately 3.9 Å is used throughout this report.) Furthermore, we have detected a Q-dependent quasielastic neutron scattering (QENS) signal in BNT, BNT-4BT and BNT-13BT. We could trace its temperature dependence in BNT-4BT down to 10 K.

Experimental Description

The samples measured were single crystals of BNT (1.0 g), BNT-4BT (8.6 g) and BNT-13BT (0.4 g). They were glued to bent Al sheet, pre-aligned, and mounted in an orange cryostat. They were aligned with the (200) and (031) reflections in the scattering plane, using fixed $k_f = 4.1\,\mathrm{Å^{-1}}$. All subsequent measurements, including the optimisation of all diaphragms, were made with fixed $k_f = 2.662\,\mathrm{Å^{-1}}$.
The first measurement on each sample was a purely elastic scan from (-0.8, 3/2, 1/2) to (1.9, 3/2, 1/2) for BNT and from (-0.8, 3/2, 1/2) to (2.25, 3/2, 1/2) for BNT-4BT and BNT-13BT, in order to verify the positions of the expected superlattice reflections at multiples of $H = 1/2$. Due to the high intensity, a "plexi" absorber with an attenuation factor of 57 had to be used in the case of BNT and BNT-4BT.
Subsequently, quasielastic scans were carried out at different Q positions. The energy transfer range was $+5$ meV to -5 meV for BNT and BNT-4BT, and $+3$ meV to -3 meV for BNT-13BT. All measurements were started at the highest energy transfer value in order to reduce the time needed for the spectrometer movement due to backlash. 13 QENS scans were measured for BNT, 13 for BNT-4BT and 2 scans for BNT-13BT. In all QENS measurements, the background was found to be significantly higher at positive than at negative energy transfer, which turned out to be the case for vanadium, too. Among the QENS measurements on BNT-4BT were scans at (0, 3/2, 1/2) and (3/2, 3/2, 1/2), measured during cooling at 300 K, 200 K, 100 K, 30 K, and 10 K.
After this, the orientation of the BNT-4BT sample was changed for measuring the phonon dispersion. This was accomplished by removing the sample from the cryostat and bending the Al sheet sample holder. The reflections (200) and (022) were used to define the scattering plane with fixed $k_f = 2.662\,\mathrm{Å^{-1}}$. In a typical series of scans along a given line in Q, the phonon dispersion was measured using 9 Q-scans ($-0.2 \leq \xi \leq 0.2$) and 11 E-scans ($+30\,\mathrm{meV} \geq \Delta E \geq 0\,\mathrm{meV}$). This was done along the following lines: (ξ, 1, 1), (2, $-\xi$, $-\xi$), ($2+\xi$, $1-\xi$, $1-\xi$), ($1+\xi$, 1, 1), (2, $1-\xi$, $1-\xi$), ($1+\xi$, $1-\xi$, $1-\xi$), with $\xi \leq 0.5$. Additional scans along ($2+\xi$, $1-\xi$, $1-\xi$) and ($1+\xi$, $1-\xi$, $1-\xi$) were measured at 100 K.

Results

The elastic scattering in Figure 1 shows the expected features for BNT: There are strong, sharp rhombohedral superlattice reflections at $H = -1/2$, 1/2, and 3/2. Furthermore, there are Al powder lines around $H = 0.6$, 1.1, and 2.25, which originate from the sample holder and the cryostat. No other maxima are visible in between. In BNT-4BT, the intensity of the rhombohedral superlattice reflections is slightly reduced, while additional peaks emerge at the tetragonal superlattice reflection positions $H = 0$, 1, and 2. These are not significantly different in BNT-13BT, whereas the rhombohedral superlattice reflections are strongly suppressed. This is intriguing since BNT-4BT is considered as possessing rhombohedral long-range order, whereas BNT-13BT is thought to be tetragonal. It appears that there exists a tetragonal order with very short correlation length in BNT, leading to diffuse streaks rather than distinct maxima. This correlation length seems to increase with low degrees of $BaTiO_3$ doping, but remain relatively constant upon a further increase of the $BaTiO_3$ concentration. On the other hand, the correlation length of the rhombohedral ordering appears relatively constant, whereas its amplitude seems to be strongly suppressed by the $BaTiO_3$ doping.

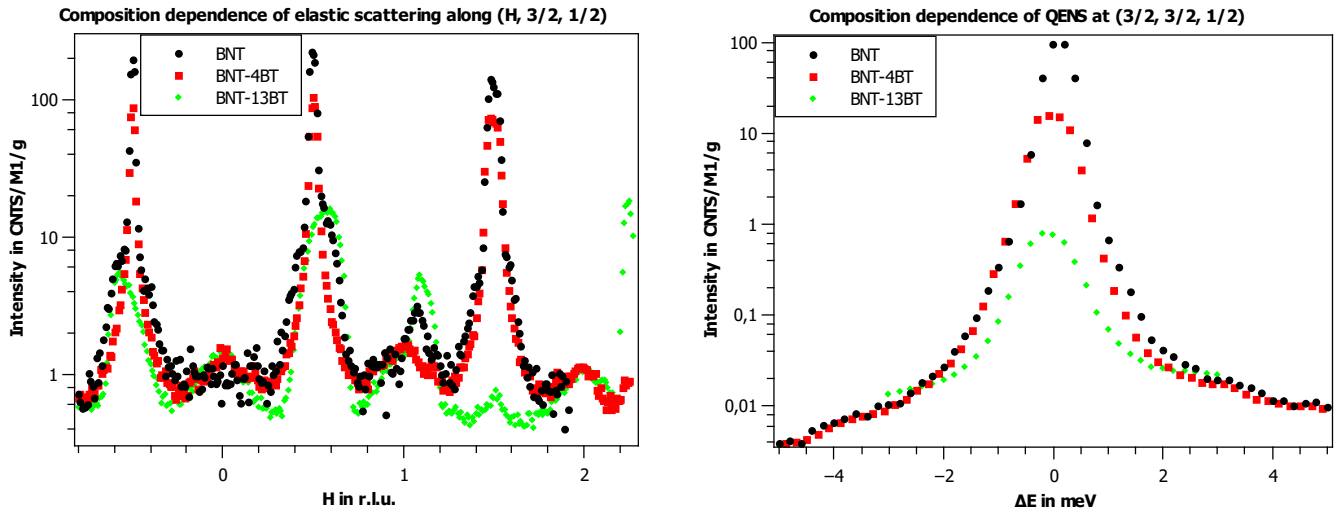

Figure 1: *Comparison of the purely elastic scattering (left) and QENS at (3/2, 3/2, 1/2) (right) in BNT, BNT-4BT and BNT-13BT. The intensity has been normalised to sample mass. The elastic scans on BNT and BNT-4BT have been corrected for additional "plexi" attenuation. The elastic peak is flattened in the QENS data of BNT-4BT due to detector saturation.*

The QENS data in Figure 1 shows a significant peak broadening at the base of all rhombohedral peaks, as do the measurements at tetragonal superlattice reflection positions (not shown). The slope of the quasielastic scattering at (3/2, 3/2, 1/2) in BNT and BNT-4BT is very similar, whereas it is significantly smaller in BNT-13BT. The intensity of the quasielastic component follows the same trend, as indicated by first fits. Since the elastic measurements have already shown the suppression of the rhombohedral ordering at high $BaTiO_3$ concentrations, the additional suppression of related dynamic features appears reasonable.

The chosen tetragonal superlattice reflection position was (1, 3/2, 1/2) for BNT and (0, 3/2, 1/2) for BNT-4BT and BNT-13BT. Thus, the BNT data may be contaminated with Al signals. On the other hand, the BNT-4BT and BNT-13BT data are considered as reliable and show a marked difference in quasielastic intensity. Although the elastic signal was very similar, the QENS intensity in BNT-13BT is significantly higher than in BNT and BNT-4BT. This indicates that the changes of the local order which result from the higher $BaTiO_3$ concentration are not of static, but dynamic nature. In contrast, the QENS intensities in BNT and BNT-4BT are relatively similar. Assuming that the Al contamination in the BNT data is purely elastic, this would indicate that the effect of the $BaTiO_3$ doping on the tetragonal ordering is mostly of static nature on the low concentration side of the MPB and mostly dynamic on the $BaTiO_3$-rich side.

Figure 2 shows that the QENS intensity is strongly temperature dependent at both superlattice reflection positions. Our first fits indicate that it is a linear function of the temperature. Only around 10 K, the background intensity starts to dominate. The linear behaviour may be due to a specific diffusive motion in which the jump distance or the excitation probability increases linearly with the temperature.

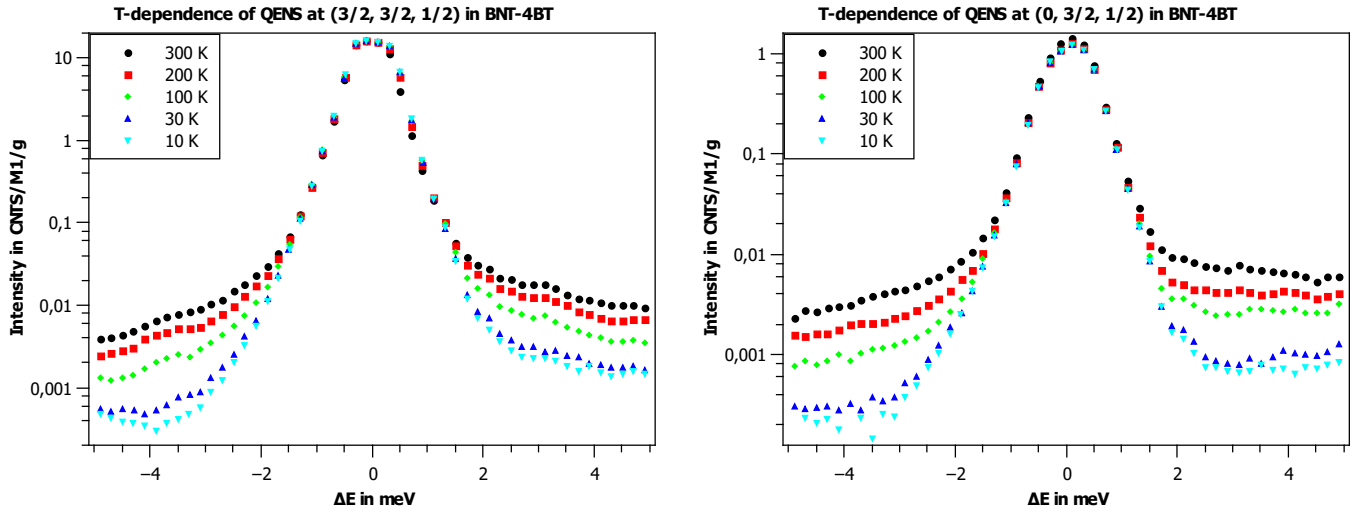

Figure 2: *Comparison of the temperature dependence of the QENS at (3/2, 3/2, 1/2) (left) and (0, 3/2, 1/2) (right) in BNT-4BT. The elastic peaks of (3/2, 3/2, 1/2) are flattened due to detector saturation. The measurements at 100 K and 30 K at (0, 3/2, 1/2) were started before the sample was in thermal equilibrium. Particularly on the positive energy transfer side, the temperature was still significantly above the respective setpoint. However, the temperature was stabilised at 30 K before the negative energy transfer side was measured.*

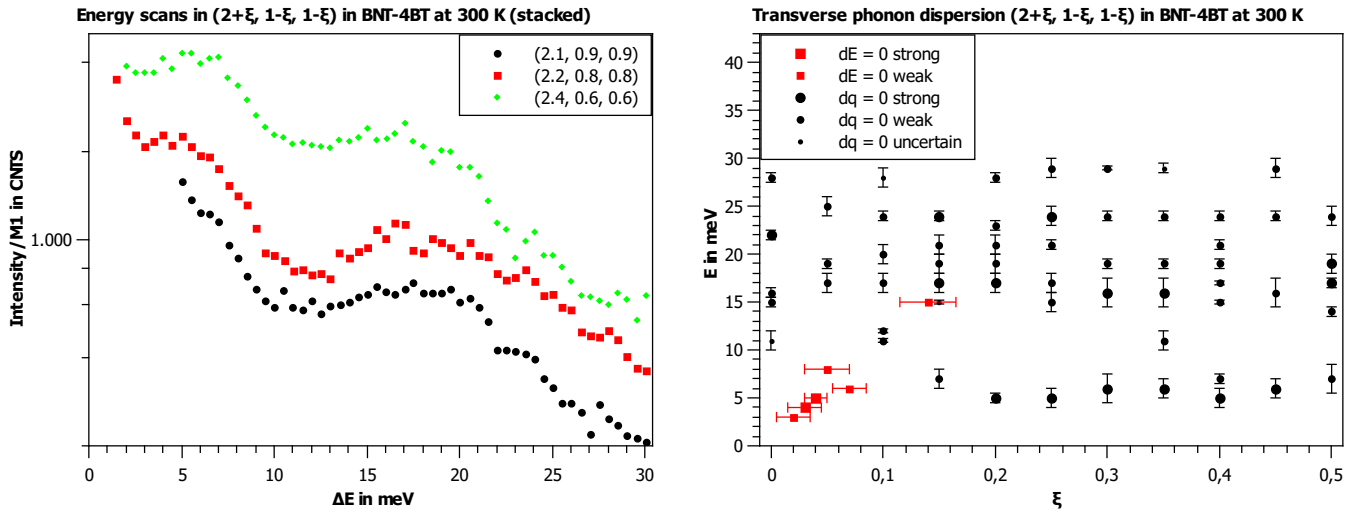

Figure 3: *Typical energy scans (left) and tentative dispersion (right) of transverse phonons in BNT-4BT at 300 K along the line $(2+\xi,\ 1-\xi,\ 1-\xi)$. The intensities of the energy scans at (2.2, 0.8, 0.8) and (2.4, 0.6, 0.6) were multiplied by a factor of $\sqrt{3}$ and 3, respectively, for easier comparison. The error bars in the dispersion indicate the estimated width of the phonon peaks. Uncertain peaks were inconclusive along $(1+\xi,\ 1-\xi,\ 1-\xi)$.*

For the construction of the phonon dispersion curves, the possible phonon peaks in all measured E and Q scans were manually classified after close inspection. Since most peaks are not well-defined, which can be clearly seen in the example in Figure 3 above, this proved to be very uncertain at times. Nevertheless, the tentative dispersion curves appear reasonable and contain some potentially very interesting features.

All dispersion curves show one clearly defined acoustic phonon branch around 6 meV. A band of optical branches can often be found between 14 meV and 20 meV. Further optical branches can appear around 12 meV and also around 25 meV. In many cases, there appears to be an unstable optical phonon branch which couples to the acoustic branch at low Q. Finally, the acoustic branch along $(2+\xi,\ 1-\xi,\ 1-\xi)$ (cf. Fig. 3) appears to possess a minimum near the zone centre at $\xi = 0.25$. This branch may well be the R_{25} phonon, which typically softens near the rhombohedral to tetragonal phase transition, but it would be surprising to see such softening behaviour 150 K below the phase transition temperature. Since, however, the minimum of the acoustic branch disappears completely at 100 K, this possibility cannot be ruled out. A further feature which disappears at 100 K is the aforementioned instability of one optical mode. Despite the low symmetry of the unit cell and high degree of disorder in the system, the phonon dispersion seems to be relatively well-ordered at low temperature. Only one acoustic phonon around 6 meV and a band of optical phonons between 15 meV and 25 meV are visible at 100 K along $(2+\xi,\ 1-\xi,\ 1-\xi)$.

Conclusion and Outlook

Our elastic and quasielastic neutron scattering data show a number of dependences of the static and dynamic correlations in BNT-BT. The static and dynamic rhombohedral ordering is clearly suppressed with increasing $BaTiO_3$ concentration. Additionally, the static tetragonal correlation seems to increase with the addition of $BaTiO_3$ only to the left of the MPB, whereas the dynamics of the tetragonal ordering increases mainly to the right of the MPB. In BNT-4BT, the dynamics of both rhombohedral and tetragonal ordering show the same temperature dependence. In both cases, it can be assumed that the amplitude or the excitation probability decrease linearly with decreasing temperature. The phonons peaks proved to be ill-defined due to the high level of disorder in the BNT-4BT sample. Nevertheless, a potential soft mode and several unstable optical modes could be identified in different directions. Both features were not observed at lower temperature.

Following our IN8 beamtime, we have extended our measurements on BNT-4BT at EIGER (SINQ). We have made elastic and quasielastic measurements at elevated temperature up to 780 K in order to trace specific features across the structural phase transitions and correlate them with the maxima of the dielectric function. We were able to show that the quasielastic scattering intensity continues to increase and dominates the elastic scattering at high temperature. We will develop a model to explain both the Q-dependence and the full temperature dependence of the QENS from 10 K to 780 K.

References

[1] J. Rödel, W. Jo, K. T. P. Seifert, E.-M. Anton, T. Granzow, and D. Damjanovic, *Journal of the American Ceramic Society,* **92** *(2009),* 1153, DOI:10.1111/j.1551-2916.2009.03061.x

[2] T. Takenaka, K. Maruyama, and K. Sakata, *Japanese Journal of Applied Physics,* **30** *(1991),* 2236, DOI:10.1143/JJAP.30.2236